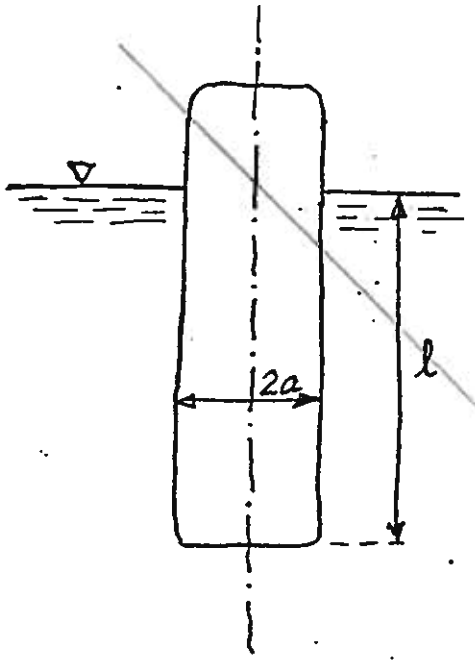

Fig. 5.27 (p. 185)

Fig. D.14. Floating vertical cylinder. The diameter is 2a and the depth of submergence is ℓ .

If $\ell >> a$, we have $m >> m_{33}$ and the angular eigen frequency is

$$\omega_o = \sqrt{S/(m+m_{33})} \approx \sqrt{S/m} = \sqrt{g/\ell} \qquad (5.328)$$

Correspondingly, the eigen period in $T_o \approx 2\pi \sqrt{g/\ell}$ which amounts to $T_o = 10s$ for a cylinder of depth $\ell = 25$ m .

Possible extension to introduction for Chapter 7 (p. 225)

Slender oscillating water column

An oscillating water column (OWC) in a narrow vertical fixed tube, as indicated in fig. D.15, may be considered as a heaving cylindrical body of water.

Then if $\ell >> a$ the eigen frequency is approximately given by $\omega_o \approx \sqrt{g/\ell}$ and the eigen period by $T_o \approx 2\pi \sqrt{\ell/g}$ which amounts to $T_o \approx 10$ s for $\ell = 25$ m

(38)

(38)

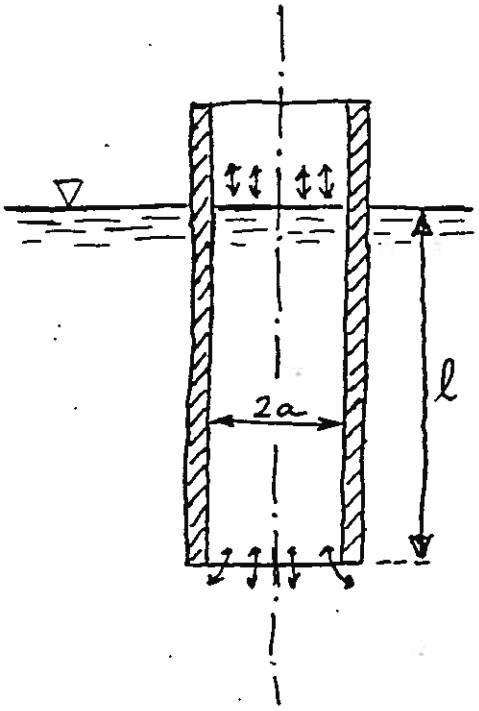

Fig. D15. A slender water column contained in a vertical open-ended tube. The diameter is 2a and the depth of submergence is ℓ . Oscillation of the water-column body may be compared with heaving oscillation of the cylinder of fig. D.14, as far as interaction with the outer sea is concerned.

The "body" of water is flexible. Hence, similar results apply for an OWC in a bended narrow tube, as shown in fig. D.16.

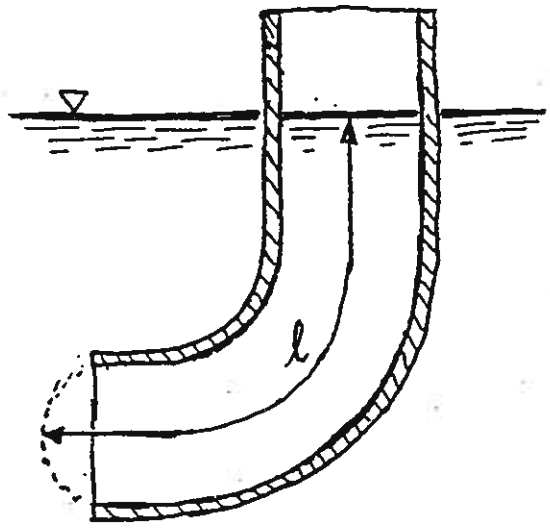

Fig. D.16. Slender water column with a bend. To make some allowance for the added-mass we may extend the envisaged column length ℓ some distance into the open sea.

(39)

(39)

We have here, as an approximation, considered an OWC as an oscillating lumpish body of water. A more correct treatment of OWC's below an entrapped air volume ~~will be~~ is given ~~later~~ in chapter ~~6~~ 7.

Extensions to Chapter 6, in particular pages 206-207 and figures 6.3 (p. 199) and 6.5 (p. 203):

D.10. PHASE CONTROL

We have seen - cf., for instance eqs. ~~[D199a]~~ (6.7) and ~~[D199b]~~ (6.18) - that in order to maximise the absorbed power or the converted useful power by means of a body oscillating in one mode, it is necessary that the velocity is in phase with the excitation force. Further, we have seen that this optimum phase condition is fulfilled if the oscillating body is in resonance with the wave. That is, the eigen (natural) frequency of the oscillating system must be equal to the actual frequency of the wave.

The oscillating position has a phase lag corresponding to a quarter period relative to the velocity, and, for a resonant oscillator, relative to the excitation force, too. For a heaving body this is illustrated by curves a and b in fig. ~~D.17~~ 6.6. Note that the amplitude of the oscillation may be larger than that of the wave. The importance of resonance is that the excitation power P_e from the incident wave to the body is never negative. In contrast, off resonance the excitation power is negative during two intervals of each cycle. During these intervals, there is a net delivery of energy from the body to the wave.

(p. 207)

Fig. 6.6

This figure (D.17) is copied from Falnes, J. & Budal, K "Wave power conversion by point absorbers", *Norwegian Maritime Research*, 6(4), pp 2-11, 1978.

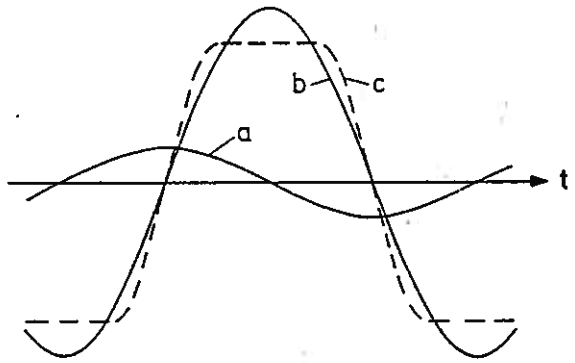

Fig. 6.17. Wave elevation and vertical displacement of a floating body as a function of time.
Curve a: Heave excitation force, which, for a slender body, is approximately in phase with the elevation of the water surface. In that case curve a also could represent the wave elevation
Curve b: Vertical displacement of body for which the oscillating mass is so large that the natural (eigen) period is equal to the wave period. (Resonance).
Curve c: Vertical displacement of body with a smaller mass, and hence shorter eigen period. As a compensation the body is latched (held in fixed position) during certain time intervals.

In order to obtain the optimum phase condition by using the principle of resonance in a practical wave-power converter, it is necessary to change the eigen frequency, for instance, by changing the mass of the oscillating body. Since the period of ocean waves typically varies over an octave, say from 6 s to 12 s, it is difficult to tune the oscillating system to resonance at all times.

Another, and even more important, problem is that real ocean waves are usually not regular. Instead the wave height and wave period vary in a stochastic manner. Then in order to obtain optimum motion it is not sufficient to tune the eigen frequency of the oscillating body to the average frequency of the wave. It is necessary to control the motion of the body on a time scale shorter than the typical wave period.

(41)

One approach, which essentially solves these difficuties in a technologically simple manner, is to use a body of so small a mass that the eigen frequency is always higher than the wave frequency, and instead provide the system with a device by which the body can be latched in fixed position during certain time intervals of the oscillation cycle. This device is controlled by an electronic system that receives input signals from wave-measuring gauges. A proper holding time is chosen to let the oscillating velocity be, as far as possible, in phase with the exciting force. Cf. fig. 6.6 D.17 where the maximum (minimum) in the derivative of curve c is synchronised with the maximum (minimum) of curve a .

Since the heaving motion (curve c) deviates from the optimum motion (curve b), the absorbed power is, in regular waves, somewhat smaller than the theoretical maximum, given by eq. (3.45 ~~[A79]~~ or (6.8 ~~[D200a]~~. However, this small deficiency is more than compensated for by the following reason. In irregular waves, where a resonant system does not perform in the optimum manner, the electronic control system can be used to adjust the length of the holding time for every individual half wave. In this way it can even in irregular waves be realised that the body moved upwards (downwards) when the body is surrounded by a wave crest (trough).

The latching mechanism may also be utilised to, intentionally, establish a non-optimum phase in situations of very high waves, in order to limit the power take-up to the actual power capacity of a practical wave energy converter.

Applying latching to obtain phase control means, even with a regular (harmonical) incident wave, and hence with a sinusoidal excitation force, that the periodic oscillatory motion contains higher harmonics. Power radiated at higher harmonics is lost without being of any use in the wave interference which is necessarily associated with wave-power absorption. A compensation for this loss is an artificial increase of the long-term (annual) average of the excitation power. This is explained as follows.

A practical wave-power converter has a finite maximum design amplitude. To be an economical device it has to operate at this oscillation amplitude a substantial part of the year, that is, at moderate wave amplitudes. As stated previously (in ~~section D.8~~ subsection 6.2.2), the radiated power is then of relatively less importance. However, the fundamental harmonic amplitude of the oscillation is (typically 20 %)[1] larger than the maximum design amplitude. In fig. ~~D.17~~ 6.6, compare curves b and c where the former is approximately equal to the fundamental harmonic of the latter.) Consequently, the excitation power with a regular incident wave is larger than that corresponding to a sinusoidal oscillation with an amplitude equal to the maximum design amplitude.

---

[1] Cf.
K. Budal, J. Falnes, L.C. Iversen, T, Hals and T. Onshus, Model experiment with a phase-controlled point absorber, 2nd International Symposium on Wave and Tidal Energy, BHRA, Bedford, UK, 1981.

The experiments described on pages 44-56 were reported in Budal, K., Falnes, J., Kyllingstad, Å. & Oltedal, G. "Experiments with point absorbers" *Proceedings of First Symposium on Wave Energy Utilization*, Gothenburg, Sweden, pp 253-282, 1979. Figures D.18, D.19, D.20, D.21, D.22, D.23 & D.24 (pages 46, 46, 49, 52, 54, 55 & 56) are copied from the same 1979 paper.

Extension to Section 6.2:

D.11. MODEL TESTS IN THE LABORATORY

We shall describe some model experiments with oscillating bodies in water waves, under conditions where viscous effects do not play an important role. Then the quantities scale according to the Froude scaling laws. Thus, the Froude number $U/(gL)^{\frac{1}{2}}$ is the same in the model as in the full-scale system. Here U and L are characteristic velocity and length, respectively. Then velocity and time scale by the length scale to the power ½, acceleration to power zero, volume, mass and force to power 3, energy to power 4, etc.

We shall give experimental results from model studies with heaving slender bodies (point absorbers). We study absorption of wave power, firstly, by resonant bodies and secondly by phase-controlled bodies, latched during parts of each wave cycle Occasionally, we also study wave generation by heaving bodies, when no incident wave is present.

The experiments have been carried out in a wave channel, 1.01 m wide and 33 m long. The water depth is $h = 1.5$ m . The side walls act as total reflectors for waves. Hence, as explained in chapter K, the experiment corresponds to an infinitely long row of bodies subject to perpendicularly, incident waves.

In the absorption experiments we use two absorbing bodies with their vertical symmetry axes placed $d = 0.50$ m apart and 0.25 m from the side walls of the channel. Since the two bodies are forced to oscillate in step with each other, we may if we wish, consider them to be one composite body. The wave period is $T = 2\pi/\omega = 1.5$ s , which corresponds to $kd = 0.91$ and $D(kh) = 1.04$.

The bodies are shaped as cylinders with hemispherical bottoms (fig. D18 and D19). The diameter is $2a = 0.15$ m , and the cylindrical part of the bodies is at equilibrium submerged to a depth of $\ell = 0.10$ m .

The heaving bodies are suspended from a wire which runs over a pulley as indicated in figs. D18 and D19. The pulley is mounted on the axis of a moving coil which can perform oscillatory motion in an adjustable magnetic field. A potentiometer mounted to the same axis serves for measurement of the vertical position of the two bodies.

In the wave generation experiment a sinusoidally varying electric current is fed to the moving coil which acts as a motor forcing the body to move up and down. In the absorption experiments the moving coil acts as an electrical generator which damps the oscillatory motion.

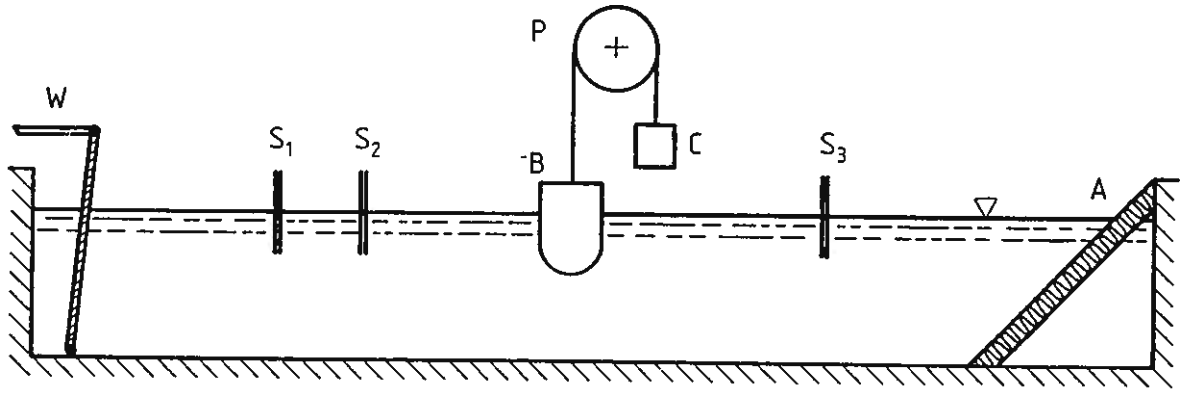

Fig. D.18. Experimental arrangement for study of heaving body (B) in wave channel. The channel comprises a wave maker (W) and an artifical beach (A). The body (B) is suspended on a flexible wire which runs over a pully (P) to an adjustable counterweight (C). The wave is measured by means of resistive two-wire probes (S_1,S_2,S_3).

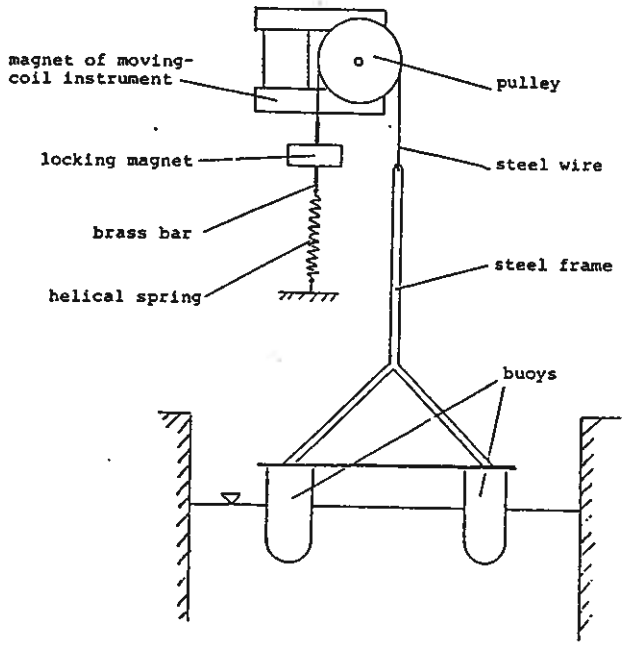

Fig. D.19. Arrangement for phase-controlled heaving bodies

In the absorption experiment with resonant bodies, tuning is obtained by adjusting the mass of the bodies and the counterweight (C in fig. D18). In the experiment with phase-controlled motion the counterweight is replaced by a locking magnet and a helical spring with its lower end at a fixed point. See fig. D19. An electronic circuit provides electric pulses to the magnet in order to lock when the speed of the body is zero at its lowest or highest position. Then the oscillatory motion is stopped until it is released by another electronic pulse approximately a time $T_o/4$ before the instantaneous heave force has a maximum or minimum, where $T_o = 0.7$ s is the natural period of the body. (Note that this period has to be shorter than the period T of the wave.) Then the body velocity is in phase with the heave excitation force, and the optimum phase condition for maximum power absorption is approximately fulfilled.

The two-wire probes S_1, S_2 and S_3 (fig. D18) are placed more than half a wavelength from the bodies in order to measure waves which are essentially plane. The probes S_1 and S_2 are interspaced $\lambda/4$ with S_1 in the antinode and S_2 in the node of the partially standing wave.

The moving-coil instrument presents to the oscillating body a mechanical load resistance R_e that is proportional to the square of the magnetic field of the instrument. In addition, there is an unavoidable loss resistance R_f which is mainly due to viscosity and to mechanical friction. Assuming that R_f is independent on the body's velocity, the (time-average) lost power is proportional to $|\hat{u}_3|^2$, the square of the velocity amplitude. The electric power converted by the coil is

(47)

(47)

$$P_u = \frac{1}{2} R_e |\hat{u}_3|^2 \qquad [D331]$$

Cf. eqs. (6.16) and (6.17).

For optimum phase ($\tau_3 = 0$), eq. ~~[D198b]~~ (6.17) gives

$$P_u = \frac{1}{2} |\hat{F}_{e,3}| \, |\hat{u}_3| - \frac{1}{2} (R_{33}+R_f) \, |\hat{u}_3|^2 = \qquad [D198d]$$

$$= \frac{1}{2} |f_3| \, |A| \omega |\hat{s}| - \frac{1}{2} (R_{33}+R_f) \omega^2 |\hat{s}|^2 \qquad [D332]$$

where $\hat{s} = \hat{u}_3/i\omega$ is the complex heave amplitude and $f_3 = \hat{F}_{e,3}/A$ is the excitation force coefficient for heave. Further, A is the complex amplitude of the incident wave at $x = 0$. It is assumed that the vertical axes of the bodies are in the plane $x = 0$.

If the magnetic field is zero, we have $R_e = 0$ and hence $P_u = 0$. For this case we have from eq. [D332] the linear relationship

$$|\hat{s}| = \frac{f_3}{\omega(R_{33}+R_f)} |A| \qquad [D333]$$

which is experimentally tested as shown in fig. D20. The agreement with linear theory is good when the heave amplitude $|\hat{s}|$ is smaller than the radius a of the body, that is, if the Keulegan-Carpenter number

$$K_C = UT/L \qquad [D334]$$

is small enough. In our case, we take as characteristic velocity, time and length $U = |\hat{u}_3| = \omega|\hat{s}|$, $T = 2\pi/\omega$ and $L = a$, respectively. Note that a is the (smallest) radius of curvature of the wetted surface. The present condition $|\hat{s}| < a$ for linear performance means that $K_C < 2\pi$.

(48) (48)

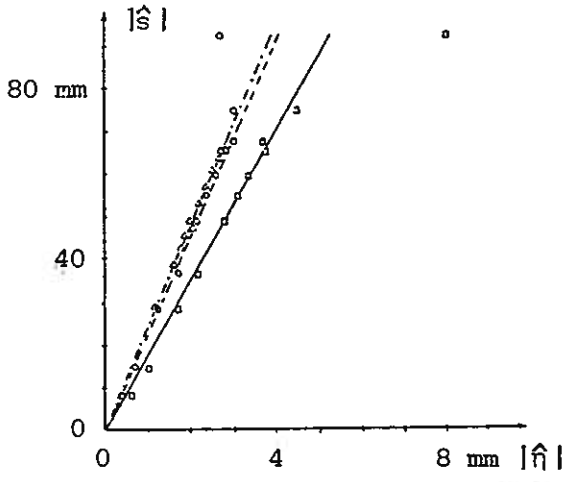

Fig. D.20. Linearity test of resonant heaving body with amplitude $|\hat{s}|$. *The fully drawn line with slope 17.5 is fitted to the measured square points representing the incident wave amplitude* $|\hat{\eta}| = |A|$. *The dashed line with slope 22.1 is fitted to the measured circle points representing the radiated wave amplitude* $|\hat{\eta}| = |\hat{\eta}_r|$. *These measurements of* $|A|$ *and* $|\hat{\eta}_r|$ *are taken under the condition of dynamical reflection (zero net load resistance,* $R_e = 0$*). The dashed-and-dotted line with slope 23.1 is fitted to the radiated wave* $|\hat{\eta}_r|$ *when the bodies are used as a wave generator.*

While eq. [D333] represents the linear relationship between the heave amplitude and the amplitude of the incident wave, we shall, as follows, derive a linear relationship between the heave amplitude $|\hat{s}|$ and the amplitude $|\hat{\eta}_r|$ of the radiated wave. Note that because of the symmetry the heaving body radiate equally large waves into the two opposite directions in the wave channel. Equating the radiated wave power transport - cf. eq. ~~[B75]~~ (4.136) - and the power delivered by the body - cf. eq. ~~[D43]~~ (6.6) - gives

$$|\hat{s}|^2 = \frac{\rho g^2 D d}{\omega^3 R_{33}^2} R_{33} |\hat{\eta}_r|^2 \qquad [D336]$$

We have here assumed that no cross waves propagate in the wave channel. Then we may use the reciprocity relation [K44c] between the radiation resistance and the excitation force

$$R_{33} = \frac{\omega |f_3|^2}{\rho g^2 D d} \qquad [D337]$$

Note that $F_{e,3}(\pi)/A = F_{e,3}(0)/A = F_3$ because of the symmetry. Combining eqs. [D336] and [D337] gives the linear relationship

$$|\hat{s}| = \frac{f_3}{\omega R_{33}} |\hat{\eta}_r| \qquad [D338]$$

Combining, further, with eq. [D33~~4~~3] shows that a fraction

$$|\hat{\eta}_r|/|A| = R_{33}/(R_{33}+R_f) \qquad [D339]$$

of the incident wave is re-radiated in the opposite direction. Under the conditions

$$ka << kd < 2\pi$$

the diffracted wave is negligible, and then it is easy to measure $|\hat{\eta}_r|$ without having a diffracted wave to correct for. However, if there were an appreciable diffracted wave to correct for, this wave could be experimentally determined in a separate measurement with the body held fixed. With negligible diffraction and with negligible friction resistance R_f compared to the radiation resistance R_{33}, eq. [D339] shows that the re-radiated wave appear, essentially as a total reflection of the incident wave. This we may term "dynamic reflection", since the phenomenon is due to a resonant slender body ($a << d$). In the downstream direction from the body the transmitted wave is almost negligible due to destructive interference between the radiated wave and the incident wave. (See fig. K5.~~4~~ - page 87)

Note that in order to avoid cross waves in the channel, the frequency must be so low that $kd < 2\pi$ (that is, $\lambda > d$). There is a possibility for propagation of an antisymmetric cross wave if $kd > \pi$, (cf. problem ~~B.2~~ 4.6). However, due to the symmetry of the present experiment, no antisymmetric cross waves are generated.

(50)

(50)

It is evident from the linearity test also of eq. [D338] that the linearity is fairly good for heave amplitudes less than the radius of the body (75 mm). See fig. D20. (Note that $|\eta_r|$ has been measured for two different situations giving essentially the same result in fig. D20. In one of those situations diffraction is not present. This demonstrates that, as was previously stated, diffraction of the incident wave is of negligible importance in the present case.) From the slopes of the fitted lines in fig. D20 we find

$$|\hat{s}| = 17.5|A| = 23|\hat{\eta}_r| \qquad [D341]$$

which means that a fraction

$$|\hat{\eta}_r/A| = 0.76 \qquad [D342]$$

of the incident wave is dynamically reflected. Further, using the experimental result [D341], we find from eq. [D336] the radiation resistance

$$R_{33} = 1.3 \text{ Nsm}^{-1} \qquad [D343]$$

Using eqs. [D339],[D342] and [D343] we find the loss resistance per body

$$R_f = 0.4 \text{ Nsm}^{-1} \qquad [D344]$$

A friction resistance of 0.2 Ns/m in the pulley has been found by a separate measurement. Hence the viscous resistance per body is $0.4 - 0.2/2 = 0.3$ Ns/m .

For the absorption experiment with phase-controlled bodies, linearity measurements are shown in fig. D21. Also here the deviation from linearity is small when the heave amplitude is less than the radius of the bodies. In this case the heave motion is non-sinusoidal but periodic. During heave motion the bodies'

position varies with time approximately as a free oscillation corresponding roughly to a cosine variation. The periodic motion is Fourier-analysed. The first harmonic amplitude $|\hat{s}_1|$ is somewhat larger than the measured amplitude s_m as indicated by the two vertical scales in fig. D21. In the linear region we have an amplitude magnification

$$|\hat{s}_1/A| \approx 10.4 \qquad [D345]$$

when there is zero electrical damping, $R_e = 0$.

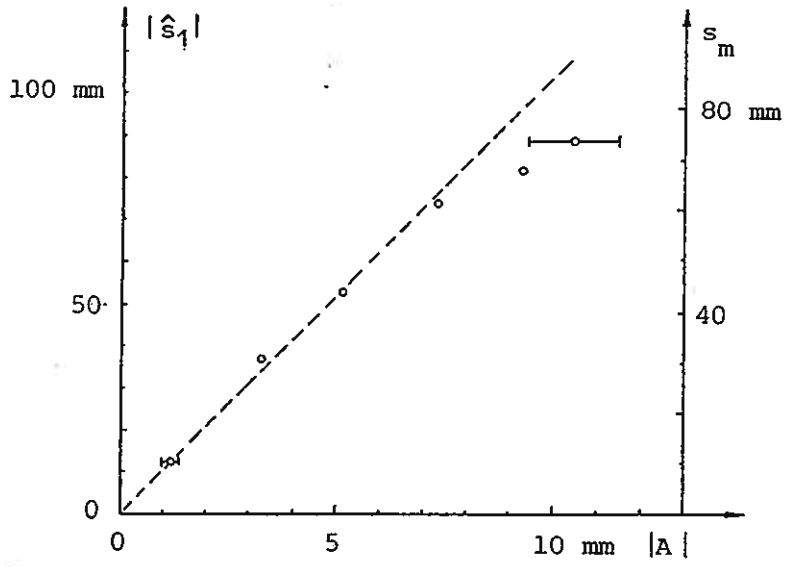

Fig. D.21. Linearity test of phase-controlled heaving body with amplitude s_m. The incident wave has amplitude $|A|$. The first harmonic amplitude of the periodic body oscillation is $|\hat{s}_1|$ as given on the left-hand vertical scale. The measurements are taken under the condition of no electrical damping, $R_e = 0$.

In comparison with eq. [D341] this indicates that the loss resistance R_f is larger than in the case of resonant bodies. Friction losses in the locking magnet, and perhaps energy losses due to non-precise latching and unlatching pulses, are partly

(52)

(52)

responsible for the increased value of R_f . Another reason is increased viscous losses due to an increased maximum heave speed. Yet another, but less important, reason is the lost power due to generated higher harmonic waves. Allowing, as before, $R_{33} = 1.3$ Ns/m the value in eq. [D345] yields an effective loss resistance

$$R_f = 1.5 \text{ Nsm}^{-1} \qquad [D346]$$

for the phase-controlled model body. In this case, a portion of the incident wave of only $|\hat{\eta}_r/A| \approx 0.46$ is dynamically reflected. Note that we disregard, here, the relatively small higher harmonical waves which result from the present phase-controlled heave motion.

When the magnetic field and hence the loss resistance R_e are varied, we obtain measured values of the electrical power P_e in the moving coil, as shown by the circle points in fig. D22. In the case of phase-controlled bodies the calculated first-harmonic amplitude $|\hat{s}_1|$ is used in the abscissa coordinate $|\hat{s}/A|$. The triangular points in fig. D22 are obtained by adding the known power loss

$$P_f = \frac{1}{2} R_f |\hat{u}_3|^2 = \frac{1}{2} \omega^2 R_f |\hat{s}|^2 \qquad [D347]$$

to the measured electrical power of the resonant bodies. In fig. D22 the power is plotted in units of incident power Jd where the wave power transport J is given by eq. ~~[B75]~~ (4.136). Fig. D22 reveals excellent agreement between theory and experiment.

(53)

(53)

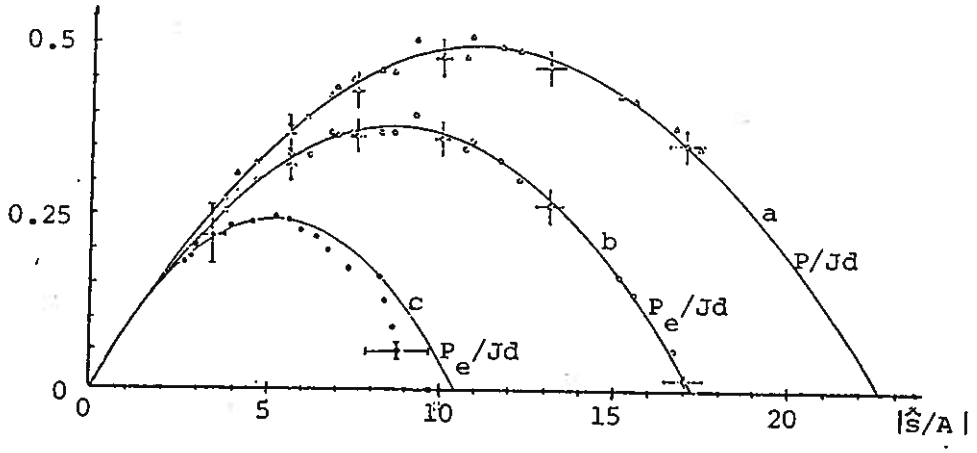

Fig. D.22. Relative absorbed power P/Jd versus relative oscillation amplitude of the heaving body. The theoretical curves represent the total absorbed power P (curve a) and the electrical power in the moving coil produced by resonant body (curve b) and by phase-controlled body (curve c). Cf. eg. [D332]. The circle points represent measured electrical power generated by the moving coil in the case of resonance. The triangular points are obtained by adding friction loss to the electrical power. The filled circle points represent electrical power in the case of phase-controlled motion.

Theoretically, one row of the heaving symmetric bodies may absorb a maximum of 50 % of the incident wave power. (Cf. section K.8.) In the present case this corresponds to a loading where the amplitude magnification is $|\hat{s}/A| = 11$. At a somewhat smaller magnification $|\hat{s}/A| = 8.7$ a maximum of 38 % of the incident wave power is converted to electrical power by the resonant point absorbers. With a magnification of $|\hat{s}/A| = 5.2$ a maximum of 25 % of the incident wave power is converted to electrical power by the phase-controlled point absorbers.

Fig. D23 shows the measured converted electrical power P_e as a function of the incident wave amplitude $|A|$. The electrical damping of the system is, in this experiment, kept constant, equal to its optimum value

(54)

(54)

$$R_e = R_r + R_f$$

i.e. $|\hat{s}| = (17.5/2)\,|A|$, in the range $|A| < 8.6$ mm or $|\hat{s}| < 75$ mm (parabolic part of curve). For $|A| > 8.6$ mm, R_e is varied in order to keep a constant heave amplitude $|\hat{s}| = 75$ mm (linear part of curve). The fully drawn, theoretical curve in fig. D23, obtained from eq. [D332], fits the experimental points fairly well.

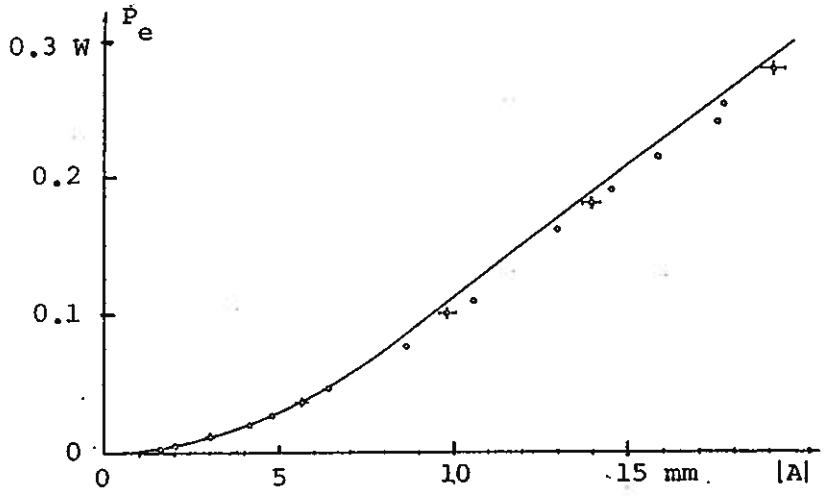

Fig. D.23. Maximum electrical power generated by one resonant body versus incident wave amplitude $|A|$. The curve is theoretical and the circular points represent measured values. For the larger values, where the curve is a straight line, the heave amplitude is restricted to $|\hat{s}| < 75$ mm.

The experiment shown in fig. D24 for bodies with phase-controlled motion is made with optimised load resistance, $R_e = R_f + R_r$. In this case there is a significant deviation from theory for large values of the wave amplitude $|A|$, when the heave amplitude exceeds the radius of the body. Thus, the deviation is due to viscous losses.

(55)

(55)

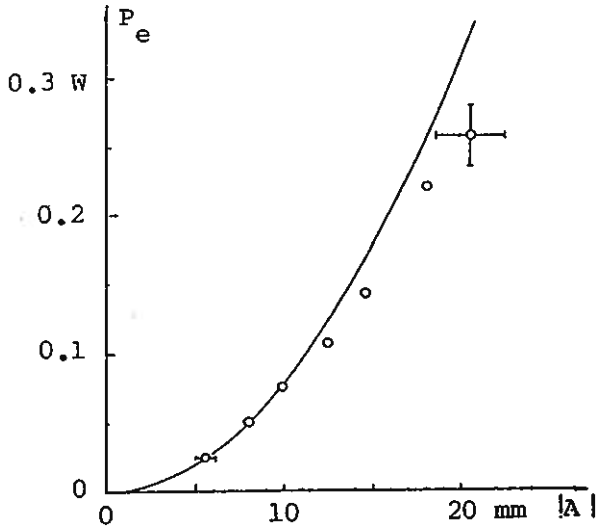

Fig. D.24. Maximum electrical power generated per phase-controlled body versus incident wave amplitude. The circles represent measured points. The curve corresponds to 26 % of the incident wave power Jd per body.

(56)

(56)

Extension to Chapter 7 (see page 229)

$$Q_{r,k} = \iint_{S_k} \frac{\partial}{\partial z} \phi_r \, dS \qquad (7.19) \quad (019)$$

Since ϕ_o and ϕ_d are linear in A and ϕ_r is linear in p_k, we have in terms of complex amplitudes, that

$$\hat{Q}_{tot,k} = \hat{Q}_{e,k} + \hat{Q}_{r,k} = q_{e,k} A - Y_{kk} \hat{p}_k \qquad (7.20) \quad (020)$$

where we have introduced the "excitation-volume-flux coefficient"

$$q_{e,k} = \hat{Q}_{e,k}/A = \iint_{S_k} \frac{\partial}{\partial z} (\hat{\phi}_o + \hat{\phi}_d)/A \, dS \qquad (7.21) \quad (021)$$

and the "radiation admittance"

$$Y_{kk} = - \iint_{S_k} \frac{\partial}{\partial z} \varphi_k \, dS \qquad (7.22) \quad (022)$$

Note that the excitation volume flux is the volume flux when the dynamic air pressure is zero ($p_k = 0$). This is a consequence of the decompositions ~~(08, 017)~~ (7.8, 7.17) which we have chosen (following D.V. Evans, 1982). Note that it is possible to choose a different decomposition (Cf. O. Malmo, A study of a multiresonant oscillating water column for wave-power absorption, Dr.ing. thesis, Institutt for eksperimentalfysikk, NTH, 1984.)

0.3. [Malmo's decomposition] Improved rigid-body description of OWC

Malmo's decomposition of the velocity potential is

$$\hat{\phi} = \hat{\phi}_o + \hat{\phi}_D + \hat{\phi}_R \qquad (023)$$

(57)

(57)

The terms satisfy

$$\nabla^2 \begin{bmatrix} \phi_o \\ \phi_D \\ \phi_R \end{bmatrix} = 0 \qquad \text{in the fluid} \tag{024}$$

$$(-\omega^2 + \frac{\partial}{\partial z}) \begin{bmatrix} \phi_o \\ \phi_D \\ \phi_R \end{bmatrix} = 0 \qquad \text{on } S_o \tag{025}$$

$$\frac{\partial}{\partial n} \begin{bmatrix} \phi_o + \phi_D \\ \phi_R \end{bmatrix} = 0 \qquad \text{on } S_b \tag{026}$$

$$\iint_{S_k} \frac{\partial}{\partial z}(\phi_o + \phi_D)\, dS = 0 \tag{027}$$

$$\iint_{S_k} \frac{\partial}{\partial z} \phi_R \, dS = Q_{tot} \tag{028}$$

Thus, this radiated wave potential is linear in the total volume flux, and the scattering (or excitation) problem correspond to zero volume flux.

Note that this description is very similar to the old rigid-piston description. However, it is modified to allow for oscillating variation of the shape of the internal water surface.

The boundary condition on S_k - (7.1, 7.13) ~~(O1, O13)~~ -

$$\hat{p}_k = (-i\omega\rho - \frac{\rho g}{i\omega} \frac{\partial}{\partial z})\hat{\phi}|_{S_k} \tag{029}$$

$$= -i\omega\rho \, \hat{\phi}|_{S_k} - \rho g \, \hat{\eta}_k \tag{030}$$

(58)

(58)

is used to define an equivalent vertical "force" on the internal water surface

$$\hat{F} = \hat{p}_k S_k = \hat{F}_E + \hat{F}_R \tag{031}$$

which is decomposed into an "excitation" part

$$\hat{F}_E = -i\omega\rho \iint_{S_k} (\hat{\phi}_o + \hat{\phi}_D) dS \tag{032}$$

and a "radiation" part

$$\hat{F}_R = -i\omega\rho \iint_{S_k} \hat{\phi}_R dS + \hat{F}_S \tag{033}$$

The last term

$$\hat{F}_S = -\rho g \iint_{S_k} \hat{\eta}_k dS = -\frac{\rho g}{i\omega} \hat{Q}_{tot} \tag{034}$$

which stems from non-zero net volume flux, corresponds to a gravitational or hydrostatic spring force. The internal water surface has an average velocity $\hat{Q}_{tot}/S_k$ and the absorbed wave power is

$$P = \frac{1}{2} \mathrm{Re}\{\hat{F}\ \hat{Q}^*_{tot}/S_k\} = \frac{1}{2} \mathrm{Re}\{\hat{p}_k\ \hat{Q}^*_{tot}\} \tag{035}$$

$$= P_E - P_R \tag{036}$$

with

$$P_E = \frac{1}{2} \mathrm{Re}\{\hat{F}_E \hat{Q}^*_{tot}/S_k\} \tag{037}$$

$$P_R = \frac{1}{2} \mathrm{Re}\{-\hat{F}_R \hat{Q}^*_{tot}/S_k\} \tag{038}$$

$$J_{k,i3} = \sqrt{G_{kk} R_{i3,i3}} \qquad (7.213)$$

We have observed that the radiation damping matrix $\underset{\sim}{A}$ is singular for a system where there is more than one mode of oscillation, for which the wave radiation is isotropic. We find a reasonable explanation for this fact, if we consider maximum wave-power absorption from a plane incident wave, as discussed in sub section ~~P1~~ 7.2.2 (see page ~~P12-20~~ 242-244), which shows that the optimum condition (7.109) [P30] represents a system of algebraic equations which is indeterminate if $\underset{\sim}{A}$ is singular. Physically, maximum power absorption is related to the maximum destructive interference between the incident plane wave and an isotropically radiated wave from the wave-power-absorbing system. A certain resulting radiated wave is required. It is, however, quite arbitrary how the various oscillator modes of the absorbing system contribute individually to the required isotropically radiated wave.

Page 258

Proof of and extension of eq. (7.29):

Extension of Section 7.2 (corresponding to extending subsection 5.5.4):

P4. POWER APPLIED BY WAVE GENERATION

In this section our main purpose is to relate the difference between average kinetic and potential energy or the reactive power to reactance parameters, such as e.g. the added-mass matrix. Cf. eqs. [P95] and [P96]. We start the derivation by considering the power applied through the oscillators by wave generation in the absence of an incident wave. This applied power is

$$P_a = \mathrm{Re}(PP_a) \qquad [P80]$$

where PP_a is the complex applied power

$$PP_a = \sum_i \iint_{S_i} \frac{1}{2}\, p v_n^* dS + \sum_k \frac{1}{2}\, p_k \iint_{S_k} (-v_z^*) dS \equiv PP_u + PP_p \quad [P81]$$

Here the two sums represent the power applied to the fluid through the N_i oscillating bodies, and through the N_k OWCs (or oscillating pressure distributions), respectively. At the integration surfaces S_i and S_k the fluid velocity has normal component

$$v_n = \partial\phi_r/\partial n \quad \text{and} \quad -v_z = -\partial\phi_r/\partial z \quad , \quad [P82]$$

respectively. The hydrodynamic pressure is

$$p = -i\omega\rho\phi_r \quad [P83]$$

According to the boundary condition ~~[P35]~~ (7.13), the applied dynamic air pressure p_k may expressed by

$$p_k = -i\omega\rho\left(1 - \frac{g}{\omega^2}\frac{\partial}{\partial z}\right)\phi_r\Big|_{S_k} \quad [P84]$$

Here the last term

$$-\frac{\rho g}{i\omega}\frac{\partial}{\partial z}\phi_r = -\frac{\rho g}{i\omega} v_z \quad [P85]$$

represents the hydrostatic stiffness of the internal water surface S_k . Using these equations in eq. [P81] we find

$$PP_a = -\frac{1}{2}\, i\omega\rho \left\{ \sum_i \iint_{S_i} \phi_r \frac{\partial}{\partial n}\phi_r^*\, dS \right.$$

$$\left. - \sum_k \left(\iint_{S_k} \phi_r \frac{\partial}{\partial z}\phi_r^*\, dS + \frac{g}{\omega^2} \iint_{S_k} \frac{\partial}{\partial z}\phi_r \frac{\partial}{\partial z}\phi_r^*\, dS \right) \right\} =$$

$$= -\frac{1}{2}\, i\omega\rho \iint_S \phi_r \frac{\partial}{\partial n}\phi_r^*\, dS - i\frac{\rho g}{2\omega} \sum_k \iint_{S_k} \left| \frac{\partial}{\partial z}\phi_r \right|^2 dS$$

(61)

(61)

Noting that the last term here is purely imaginary, we find that the applied power is

$$P_a = \mathrm{Re}(PP_a) = \frac{1}{2}\,(PP_a + PP_a^*) = \frac{i\omega\rho}{4}\, I(\phi_r^*, \phi_r) \qquad [P86]$$

where I is given by the integral ~~[P59]~~ (4.240) or ~~[P61]~~ (4.243). Using eqs. ~~[P38]~~ (7.113) (7.140), (7.153) and (7.164) and ~~[P62]-[P64]~~ in [P86] and comparing with eq. ~~[P25]~~ (7.99) it is seen that $P_a = P_r$ which is reasonable, since in an ideal fluid with no energy dissipation the applied power must be equal to the radiated power.

Further, from eq. [P81] we find the applied reactive power

$$\mathrm{Im}(PP_a) = \frac{1}{2i}\,(PP_a - PP_a^*) =$$

$$= -\frac{\omega\rho}{4} \iint_S \left(\phi_r \frac{\partial}{\partial n}\phi_r^* + \phi_r^* \frac{\partial}{\partial n}\phi_r\right) - \frac{\rho g}{2\omega} \sum_k \iint_{S_k} \left|\frac{\partial}{\partial z}\phi_r\right|^2 dS =$$

$$= -\frac{\omega\rho}{4} \iint_S \frac{\partial}{\partial n}\left|\phi_r\right|^2 dS - \frac{\rho g}{2\omega} \sum_k \iint_{S_k} \left|\frac{\partial \phi_r}{\partial z}\right|^2 dS \qquad [P87]$$

which we shall relate to the energy stored in the near-field of the radiating oscillators.

The time-averaged kinetic energy of the fluid domain τ contained within the control cylinder S_∞ (fig. ~~P1~~ 7.1) is

$$T = \frac{\rho}{2} \iiint_\tau \frac{1}{2}\, v\, v^*\, d\tau = \frac{\rho}{2} \iiint_\tau \frac{1}{2}\, \nabla\phi_r \cdot \nabla\phi_r^* d\tau \qquad [P88]$$

By using the Laplace equation and the homogeneous boundary conditions ~~[P33]-[P34]~~ (7.114) - (7.115) for ϕ_r and the divergence theorem, we obtain

$$T = \frac{\rho}{4} \iint_{S_\infty} \phi_r \frac{\partial}{\partial r}\phi_r^* dS - \frac{\rho}{4} \iint_S \phi_r \frac{\partial}{\partial n}\phi_r^* dS + V_o \qquad [P89]$$

where

$$V_o = \frac{\rho\omega^2}{4g} \iint_{S_o} \phi_r \phi_r^* dS = \frac{1}{2} \rho g \iint_{S_o} \frac{1}{2} \eta\eta^* dS \qquad [P90]$$

is the time-averaged potential energy due to the elevation η of the free water surface S_o external to bodies and chambers. Cf. fig. ~~P1~~ 7.1 and eq. ~~[B83e]~~ (4.119) (p. ~~B27~~ 76).

At large distance, where asymptotic expressions like ~~[P65]~~ ~~[P74]~~ (7.190) apply, the contribution to $T - V_o$ is negligible if the radius r of the control cylinder is increased, since it can be shown that the surface density of $T - V_o$ is $O(kr)^{-3/2}\}$ as $kr \to \infty$. Thus, in the far-field region a propagating wave is associated with a time-averaged energy (per unit horizontal surface) of $(\rho g/2)\eta\eta^*$ which is equally partitioned between kinetic energy and potential energy. Cf. eq. ~~[B85] (p.29)~~ (4.128). Hence, a non-vanishing difference between kinetic energy and potential energy is associated with reactive power in the near-field region. Using eq. ~~[P61]~~ (4.243) or eq. ~~[D117] (p. B50)~~ (4.240) in eq. [P89] we obtain

$$T - V_o = \frac{\rho}{4} \left\{ \iint_{S_\infty} \phi_r \frac{\partial}{\partial r} \phi_r^* \, dS - \frac{1}{2} I\{\phi_r, \phi_r^*\} \right\}$$

$$+ \frac{\rho}{8} \iint_S \left(\phi_r \frac{\partial}{\partial n} \phi_r^* - \phi_r^* \frac{\partial}{\partial n} \phi_r \right) dS - \frac{\rho}{4} \iint_S \phi_r \frac{\partial}{\partial n} \phi_r^* \, dS$$

Since the velocity potential ϕ_r satisfies the radiation condition, the first of these terms vanishes, in accordance with eq. ~~[D135e] (P. B56)~~ (4.255), provided the radius r of the control

cylinder S_∞ tends to infinity. Moreover, the two last integrals may be joined into one integral over S where the integrand is $(\rho/8)(\partial/\partial n)(-\phi_r\phi_r^*)$. Hence, assuming that the control cylinder is in the far-field region ($r \to \infty$), we have

$$T - V_o = -\frac{\rho}{8}\iint_S \frac{\partial}{\partial n}\left|\phi_r\right|^2 dS \qquad [P91]$$

Next, we consider the contribution V_k to the potential energy from the vertical displacement

$$\eta_k = -\frac{p_k}{\rho g} - \frac{i\omega}{g}\phi_r\Big|_{z = z_k} \qquad [P92]$$

of the internal water surface S_k. Cf. eq. ~~[B32a] (p. B14)~~ (4.40). Since eq. ~~[B83c] (p. B27)~~ (4.119) for the surface density of the potential energy, is applicable also in the present case, we have

$$V_k = \frac{1}{2}\rho g\iint_{S_k}\frac{1}{2}\eta_k\eta_k^* dS = \frac{\rho}{4}\iint_{S_k}\left\{\frac{\omega^2}{g}\left|\phi_r\right|^2 + \frac{i\omega}{\rho g}(p_k^*\phi_r - p_k\phi_r^*) + \frac{\left|p_k\right|^2}{\rho^2 g}\right\}dS \qquad [P93]$$

In the last integral, the first term is due to gravity and the third term represents hydrostatic energy, while the second term is a coupling term.

The total time-averaged potential energy is

$$V = V_o + \sum_k V_k \qquad [P94]$$

Using the boundary condition ~~[P35]~~ (7.13 & 7.149, 7.125) for ϕ_r the last term in eq. [P87] may be rewritten as

$$-\frac{\rho g}{2\omega}\sum_k\iint_{S_k}\frac{\partial}{\partial z}\phi_r\frac{\partial}{\partial z}\phi_r^* dS =$$

$$- \frac{\rho g}{2\omega} \sum_k \iint_{S_k} \left(\frac{\omega^2}{\rho g}\,\phi_r - \frac{i\omega}{\rho g}\,p_k\right)\left(\frac{\omega^2}{\rho g}\,\phi_r^* + \frac{i\omega}{\rho g}\,p_k^*\right) dS =$$

$$- \frac{\rho\omega}{2} \sum_k \iint_{S_k} \left\{\frac{\omega^2}{g}\,\phi_r\phi_r^* + \frac{i\omega}{\rho g}\left(p_k^*\phi_r - p_k\phi_r^*\right) + \frac{1}{\rho^2 g}\,p_k p_k^*\right\} dS =$$

$$- 2\omega \sum_k V_k$$

Further, using also eqs. [P91] and [P94] in eq. [P87] we find that the reactive applied power is

$$\mathrm{Im}(PP_a) = 2\omega(T-V) \qquad [P95]$$

For a transmitting antenna an analogous expression exists for reactive electrical power in terms of the difference between magnetic and electric energy. A simpler analogue is an ordinary damped oscillator as discussed in chapter ~~A~~ 2, section ~~A4~~ 2.3. At resonance, stored energy is alternating between kinetic energy and potential energy, both of which have the same time-averaged value, while the reactive power is zero, since only active power (P_a) has to be applied to the oscillator. Off resonance, however, a non-vanishing reactive power has to be applied, since there is no longer balance between the time-averaged values of the two kinds of stored energy.

Using the decomposition ~~[P38]~~ (7.113) for the radiated velocity potential ϕ_r and the expressions ~~[P62]~~ (7.151), ~~[P63]~~ (7.140), ~~[P64]~~ (7.162) and ~~[P56]~~ (7.160) for the radiation damping parameters we may show from eq. [P86] that the applied power P_a equals the radiated power P_r as given by eq, ~~[P26]~~ (7.100), $P_a = P_r$. Correspondingly, the complex applied power equals the complex radiated power, $PP_a = PP_r$, which we shall prove

as follows. The contributions to the complex applied power PP_a from the oscillating bodies and from the OWCs are

$$PP_u = -\frac{1}{2}\, i\omega\rho \sum_i \iint_{S_i} \phi_r \frac{\partial}{\partial n} \phi_r^* \, dS$$

and

$$PP_p = \frac{1}{2}\, i\omega\rho \sum_k \iint_{S_k} \left(\phi_r \frac{\partial}{\partial z} \phi_r^* - \frac{g}{\omega^2} \frac{\partial}{\partial z} \phi_r \frac{\partial}{\partial z} \phi_r^* \right) dS$$

respectively. Using, firstly, the boundary condition ~~[P35]~~ (7.13) and the decomposition ~~[P38]~~ (7.113) for the radiated velocity potential ϕ_r and, secondly, the expressions, ~~[P49]~~ (7.132) and ~~[P50]~~ (7.133) for the radiation parameters $Y_{k,k'}$ and $H_{k,ij}$ we find

$$PP_p = \frac{1}{2}\, i\omega\rho \sum_k \iint_{S_k} \frac{i}{\rho\omega} p_k \left(\sum_{k'} \frac{\partial}{\partial z} \varphi_{k'}^* p_{k'}^* + \sum_{ij} \frac{\partial}{\partial z} \varphi_{ij}^* u_{ij}^* \right) dS$$

$$= -\frac{1}{2} \sum_k p_k \left(-\sum_{k'} Y_{k,k'}^* p_{k'}^* - \sum_{ij} H_{k,ij}^* u_{ij}^* \right)$$

Moreover, using, firstly, the decomposition ~~[P38]~~ (7.113) and the boundary conditions, ~~[P44]~~ (7.116) and ~~[P45]~~ (7.117), secondly the expressions ~~[P53]~~ (7.128), [P54] (7.129) and ~~[P56]~~ (7.160) for radiation parameters, we rewrite PP_u as

$$PP_u = -\frac{1}{2}\, i\omega\rho \sum_i \iint_{S_i} \left(\sum_k \varphi_k p_k + \sum_{i'j'} \varphi_{i'j'} u_{i'j'} \right) \sum_j u_{ij} u_{ij}^* \, dS$$

$$= \frac{1}{2} \sum_{ij} \left(-\sum_k H_{k,ij} p_k + \sum_{i'j'} Z_{ij,i'j'} u_{i'j'} \right) u_{ij}^*$$

Using the last expression for PP_p and for PP_u we find that $PP_a = PP_u + PP_p = PP_r$ where PP_r is given by eq. ~~[P25]~~ (7.99). Taking the imaginary part of eq. ~~[P25]~~ (7.99) and using eq. [P95] then give

$$T - V = \frac{1}{2\omega} \left(\frac{1}{2} \tilde{u}_{NN} X u^* - \frac{1}{2} \tilde{p}_{NN} B p^* - \mathrm{Re}\{ \tilde{p}_{NN} J u^* \} \right) \qquad [P96]$$

This expression is an extension of a previously known formula involving the added mass matrix $\underset{\sim}{X}/\omega$. (Cf. McIver and Evans, Journal of Engineering Mathematics, Vol 8, pp. 7-22, 1984.)

In a case with only OWCs and no oscillating bodies, we have

$$\frac{1}{4}\,\tilde{\underset{\sim}{p}}(\underset{\sim}{B}/\omega)\underset{\sim}{p}^{*} = V - T \qquad [P97]$$

Since we use the term added mass even if it is not associated with kinetic energy only, we could term $\underset{\sim}{B}/\omega$ the "added compliance" matrix in spite of the fact that it is not associated with potential energy, only.

Note that $\underset{\sim}{B}/\omega$ contains the effect of buoyancy of the oscillating internal water surfaces corresponding to the hydrostatic potential energy. This contribution

$$\underset{\sim}{B}_{O}/\omega = \mathrm{diag}\{S_k/\rho g\} \qquad [P98]$$

to B/ω corresponds to the last term in eq. [P93]. It is reasonable to assume that no wave is generated in the limit of zero frequency, which means that $\phi_r \to 0$ as $\omega \to 0$. Then there is no contribution to $V - T$ other than the hydrostatic potential energy. In fact, it follows from eqs. ~~[P41]~~ (7.119) and ~~[P49]~~ (7.132) that

$$Y = i\underset{\sim}{B}_{O} + o(\omega) \quad \text{and} \quad \underset{\sim}{G} = o(\omega) \to 0 \quad \text{as} \quad \omega \to 0 \qquad [P99]$$

For one single OWC in a circular vertical tube with radius a eq. [P98] gives $B_O/\omega = \pi a^2/\rho g$ in accordance with a previously known zero-frequency limit of B/ω (Cf. chapter ~~0~~ 7, fig. ~~03~~ 7.3, p. ~~011~~ 231). Arguing similarly we find the following zero-frequency limit for the excitation volume flux coefficient

$$q_k = Q_k/A_k \to i\omega S_k \quad \text{as} \quad \omega \to 0 \qquad [P100]$$

(See eq. ~~[052]~~ (7.34) (p. ~~09~~ 231).)